# The Impact of Recent High-Resolution Global Digital Elevation Models to the Determination of Basin Hydrological Properties. An Application to Northern Greece

Eleni A. Tzanou[1] and Georgios S. Vergos[2]

[1]*Technological Educational Institute of Serres, Department of Geomatics and Surveying, Faculty of Applied Technology, Greece;*
*etzanou@yahoo.com*

[2]*Aristotle University of Thessaloniki, Department of Geodesy and Surveying, Greece;*
*vergos@topo.auth.gr*

**Abstract.** The combined use of Geographic Information Systems and recent high-resolution Digital Elevation Models (DEMs) from Remote Sensing imagery offers a unique opportunity to study the hydrological properties of basin and catchment dynamics and derive the hydrological features of specific regions of various spatial scales. Until recently, the availability of global DEMs was restricted to low-resolution and accuracy models, e.g., ETOPO5, ETOPO2 and GTOPO30, compared to local Digital Terrain Models (DTMs) derived from photogrammetric methods and offered usually in the form of topographic maps of various scales. The advent of the SRTM and ASTER missions, offer some new tools and opportunities in order to use their data within a GIS, to study the hydrological properties of basins and consequently validate their performance both amongst each other, as well as in terms of the results derived from a local DTM. The present work focuses on the use of the recent SRTM v2 90 m and ASTER v2 30 m DEMs along with the national 500 m DTM generated by the Hellenic Military Geographic Service (HMGS), within a GIS in order to assess their performance in determining the hydrological properties of basins. To this respect, the Spatial Analyst and 3D Analyst extension tools of ArcGIS v9.3, HEC-RAS v4.1 and RiverCAD have been exploited to determine the hydrographic data of the basins under study which are located in Northern Greece. The hydrological characteristics refer to stream geometry, curve number, flooding areas, etc. as well as the topographic characteristics of the basin itself, such as aspect, hillshade, slope e.t.c..

**Keywords.** ASTER, DEMs, hydrology, satellite models, floods, SRTM.

## 1. Introduction

The study of basin hydrological and hydraulic characteristics has relied heavily during the past years on field topographic work, given that the available global digital terrain and digital elevation models (DTMs and DEMs, respectively) presented low spatial resolution and contained voids. Given the time-consuming and cumbersome nature of field-surveying, such applications referred only to small catchment areas. Moreover, the limited spatial resolution of global DEMs, such as ETOPO5, ETOPO2 and GTOPO30, prohibited their use for local and regional applications, since they could not represent the fine details of the topography. Their limited accuracy on the other hand could result in biased estimates about the hydrological properties of basins and thus inaccurate estimations. Both aspects play a crucial role mainly to the extraction of the morphological characteristics of the area under study, such as the derived slope, which in itself biases consequently the basin delineation, stream geometry, flow direction, etc. [1].

This problematic situation improved significantly when, in 2000, the Shuttle Radar Topographic Mission (SRTM) was launched on-board space shuttle Endeavour and collected a wealth of data of the Earth's topography in a global scale and with homogeneous coverage [2], [3], [4], [5]. This resulted in the release of a global 3″ (roughly 90 m) SRTM DTM by NASA and the National Geospatial-Intelligence Agency (NGA). From the SRTM data resolution and the estimated horizontal and vertical accuracy (95% linear error) of ±7.8 m and ±6.2 m, respectively [6], it became obvious that such a global DEM could offer great aid to local and regional hydrologic modelling and possibly make the necessity of local field surveys obsolete [7], [8]. It should be noted that the satellite models like SRTM are all digital elevation models or better digital surface models (DSMs) in the sense that they provide the height of the Earth's topography, including vegetation in rural areas and buildings in urban ones, above some reference surface (geoid, ellipsoid, etc.). To this respect, it should always be acknowledged that they do not represent the actual land topography of the Earth and that in all cases the SRTM elevations inherit problems due to mountain shadowing and roof-top effects.

In December 1999, the Terra satellite was launched in the frame of the NASA Earth Observation System (EOS) program, which carried on-board the ASTER Advanced Spaceborne Thermal Emission and Reflectance Radiometer (ASTER) sensor [9]. Its main goal was the collection of data for versatile constituents like cloud cover, temperature, land use and land cover, vegetation, etc. One of its products refers to a global DEM with an unprecedented resolution at a global scale of 1″ (roughly 30 m), with its second release being issued in October 2011. Its formal vertical root mean square error is at the ±8.6 m with an absolute accuracy (95% linear error) of ±18.3 m and the horizontal error is at the ±16.8 m. As in the SRTM case, ASTER elevation models are in sense DEMs rather than DTMs. It is worth mentioning that the determination of elevation from Lidar is gaining increasing attention in related studies [4], [1], since it provides height data with high spatial resolution and in a timely fashion, but the financial aspects of the method is its main limitation, while on the other hand satellite data are freely available.

Given the availability of these two global DEMs, which represent the varying topography of the Earth with unprecedented resolution at global scales, the aim of the present work is to utilise their height information in order to derive the hydrological and hydrographic characteristics of a medium-sized catchment area in Northern Greece, concentrating in the drainage basin of river Kosynthos in Thrace, Greece. As a ground truth dataset, against which the results derived by the two global DEMs will be validated, a local DEM derived from the digitisation of topographic maps (1:50000 and 1:5000 scale) from the Hellenic Geographic Military Service (HMGS) has been used. The latter has been augmented with elevations acquired in a dedicated filed topographic survey, which was carried out to a length of 12.5 km across the main river in the area and to a zone of 1.1 km from the river crest. To reach that goal, first the available DEMs have been compared to each other and then the necessary topographic characteristics for the hydrological analysis, like slope and aspect, have been derived [4], [10], [11], [12]. Then, the basin delineation has been carried out and the hydrological characteristics have been determined, referring to stream geometry, curve number, flooding areas and flow accumulation. All necessary processing has been carried out using the Spatial Analyst and 3D Analyst extension tools of ArcGIS v9.3, HEC-RAS v4.1 and RiverCAD [13], [8], [14].

## 2. Data availability, the catchment area under study and DEM evaluation

The area under study is bounded between $41.0° \leq \varphi \leq 41.5°$ and $24.6° \leq \lambda \leq 25.2°$ and is located in the Kosynthos River close the city of Xanthi, approximately 2.5km away from its outflow in the Vistonida Lake (Figure 1). In order to cover a wider part of the area under study and avoid edge

effects, the data from SRTM and ASTER were composed by four tiles each with a 1°×1° spatial extend to both latitude and longitude. Given that the second releases (v2) of both mission have been available, they were used compared to release 1 of both mission data, since they provide improved horizontal and vertical accuracies. It should be mentioned that the satellite data geographic coordinates refer to WGS84, hence they were transformed to the Hellenic Geodetic Reference System 1987 through appropriate geodetic transformation from the WGS84 to the GRS80 ellipsoid. Given that the local topographic maps of scale 1:50000 and 1:5000 were available in projected coordinates, the satellite data have been subsequently transformed to local Transverse Mercator 1987 (TM87) easting and northing cartesian coordinates.



Figure 1: The area under study in Northern Greece.

As a first pre-processing step for the satellite data, all voids indicating blank areas have been removed and prediction with a kriging interpolation has been carried out to fill-in blanks. For the kriging interpolation, the necessary empirical variances for the variograms have been computed with an input error set equal to the inverse of the elevation of the 200 nearest points. This resulted in a complete mesh of elevations for both SRTM and ASTER, from which the respective tin surfaces have been determined. The same procedure has been followed for the local HMGS DEM with the exception that in this case the available contour lines in the topographic maps have been digitised, then augmented with the local survey data and then integrated to generate the HMGS tin. Figures 2, 3 and 4 depict the tin surfaces from the three available models, where the influence of their varying resolution can be seen in the final result.

In order to assess the performance of the satellite DEMs, a direct comparison between them and to the local HMGS model has been performed. Given that the ASTER model has the highest spatial resolution, elevations from that model have been interpolated to the grid points where data from the other models were available. Table 1 summarizes the statistics of the available DEMs as well as their differences. From that Table it can be concluded that the satellite models sample the same

elevation amplitudes since their range is approximately the same with a maximum elevation of 1819 m
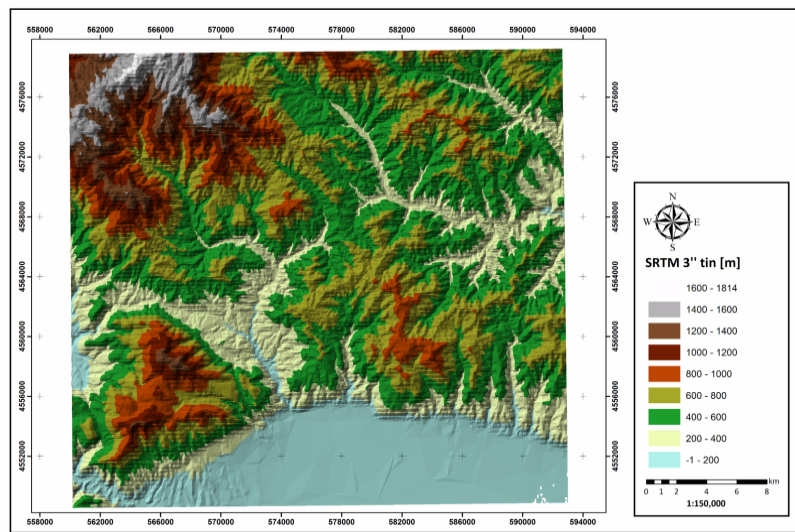


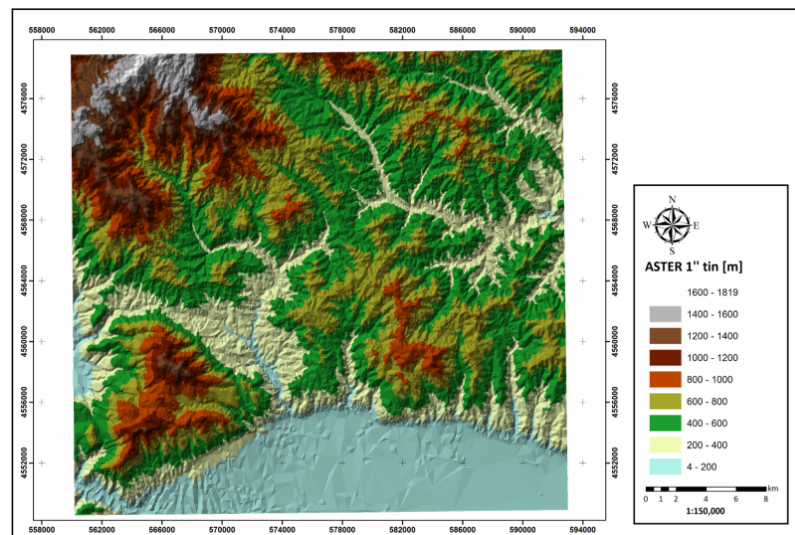Figure 2: The SRTM v2 tin surface in the area under study.



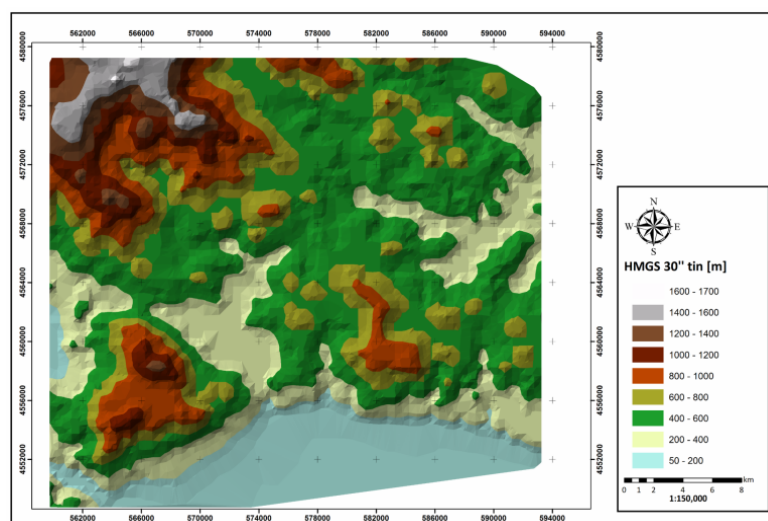Figure 3: The ASTER v2 tin surface in the area under study.



Figure 4: The HMGS tin surface in the area under study.

**Table 1**: Statistics of the available HMGS (local), ASTER and SRTM DEMs and their comparison.

| DEMs | | | | | |
|---|---|---|---|---|---|
| | max | min | mean | rms | std |
| HMGS | 1715.000 | 1.000 | 535.975 | ±633.048 | ±336.868 |
| ASTER 1″ | 1819.000 | 4.000 | 536.679 | ±633.562 | ±336.715 |
| SRTM 3″ | 1814.000 | 0.000 | 542.193 | ±638.759 | ±337.698 |
| DEM Differences | | | | | |
| HMGS-SRTM | 249.000 | -286.000 | -9.454 | ±53.621 | ±52.781 |
| HMGS-ASTER | 210.992 | -222.164 | 1.047 | ±47.913 | ±47.902 |
| ASTER-SRTM | 164.875 | -136.063 | -6.060 | ±22.522 | ±21.691 |

for ASTER and 1814 m for SRTM. On the contrary, the local model has a maximum value of 1715 m, which is 100 m smaller than the one from the satellite models. Even though the satellite models agree in the range of the elevations, they mean value of the ASTER DEM is almost identical to that of the local model, 537 m, compared to the one by SRTM which deviates by ~7 m. This behavior of the latter can indicate a possible bias of the order of 7 m in the area under study, which can therefore influence to some extent the derived hydrographic characteristics.

To quantify the differences between the available models, their differences have been plotted as well in order to identify possible spatial patterns. The statistics of the differences are presented in Table 1 (last three rows), while Figures 5, 6 and 7 depict their spatial distribution in the area under study. The differences between HMGS and the ASTER DEM are at the ±47.9 m level (1σ) with a mean value at the 1 m only. This indicates that the ASEM model, at least from its comparison with the local data, contains no biases, while the range of the differences is at the 430 m level. Contrary to that, the SRTM DEM has a bias of the order of -9.5 m compared to the local one, while the range is larger as well and reaches the 535 m with a standard deviation of ±52.8 m. From Figure 5, where the differences between the HMGS and SRTM models are depicted, a spatial pattern from the SW to the NE direction is visible, while we can conclude that the variation of the difference is significant as well. The differences between HMGS and ASTER are much smoother (Figure 6) with smallest variations and no obvious spatial patterns. The influence of this bias in the SRTM data can be seen as well in Figure 8, where the histograms of the differences are depicted. From the histograms it can be seen that the one between ASTER and HMGS show a normal distribution with small side-lobes, while the ones between SRTM and HMGS have larger side-lobes with smaller concentration within a 1σ and 2σ region and an obvious bias since they are off-centered relative to zero. When investigating the range between -40 and +40 m for the computed differences, only 54% of those between ASTER and HMGS are out of these limits while the percentile rises to an 84% for the ones between HMGS and SRTM. Quite interesting is the histogram of the differences between ASTER and SRTM as well, where it can be seen that a large amount (42.5%) of the differences are on the negative side between -2 and 36 m.

Given the analysis of the available DEMs presented in this section, the computed tin surfaces have been used to derive some basic topographic characteristics for the area under study, like slope

and aspect. Slope is an integral part in the determination of hydrological characteristics, since errors in the DEM will propagate the estimation of the slope as well.
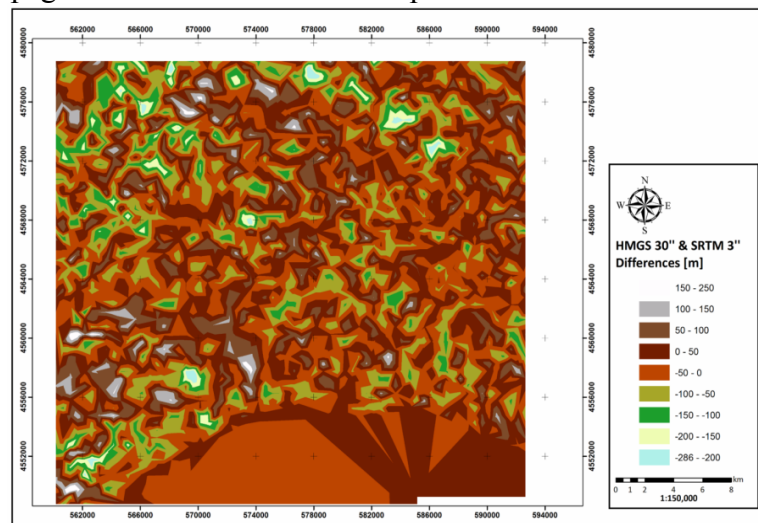
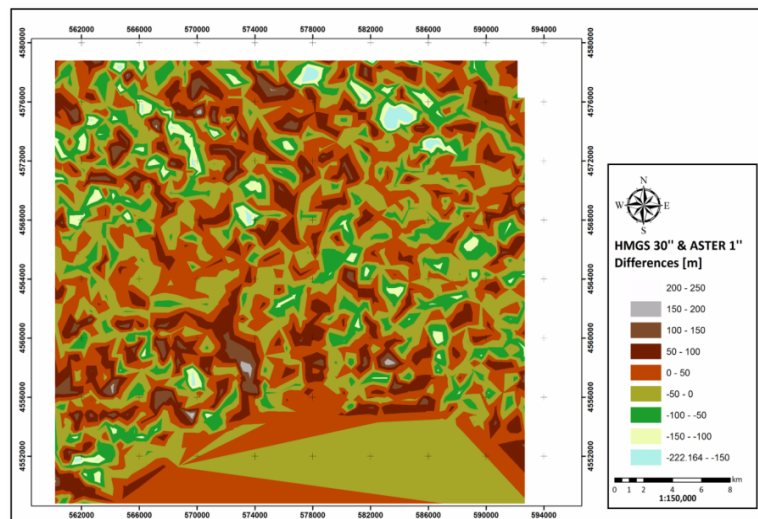Figure 5: Differences between the HMGS and SRTM v2 DEMs in the area under study.

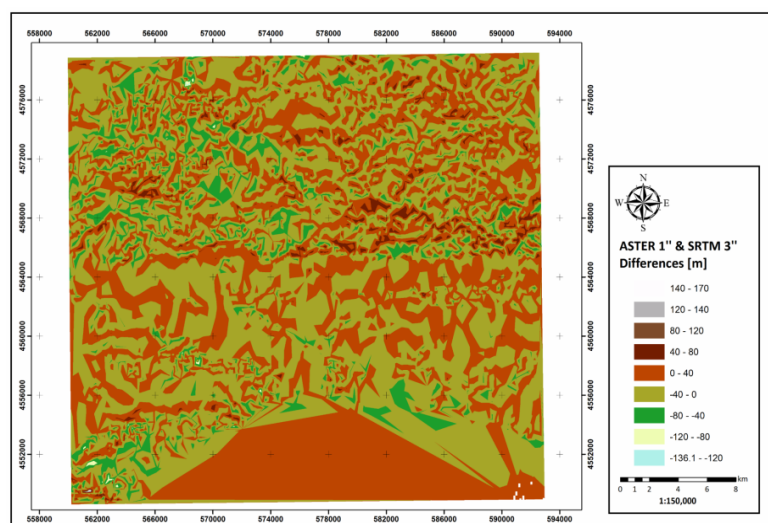Figure 6: Differences between the HMGS and ASTER v2 DEMs in the area under study.

Figure 7: Differences between the ASTER v2 and SRTM v2 DEMs in the area under study.
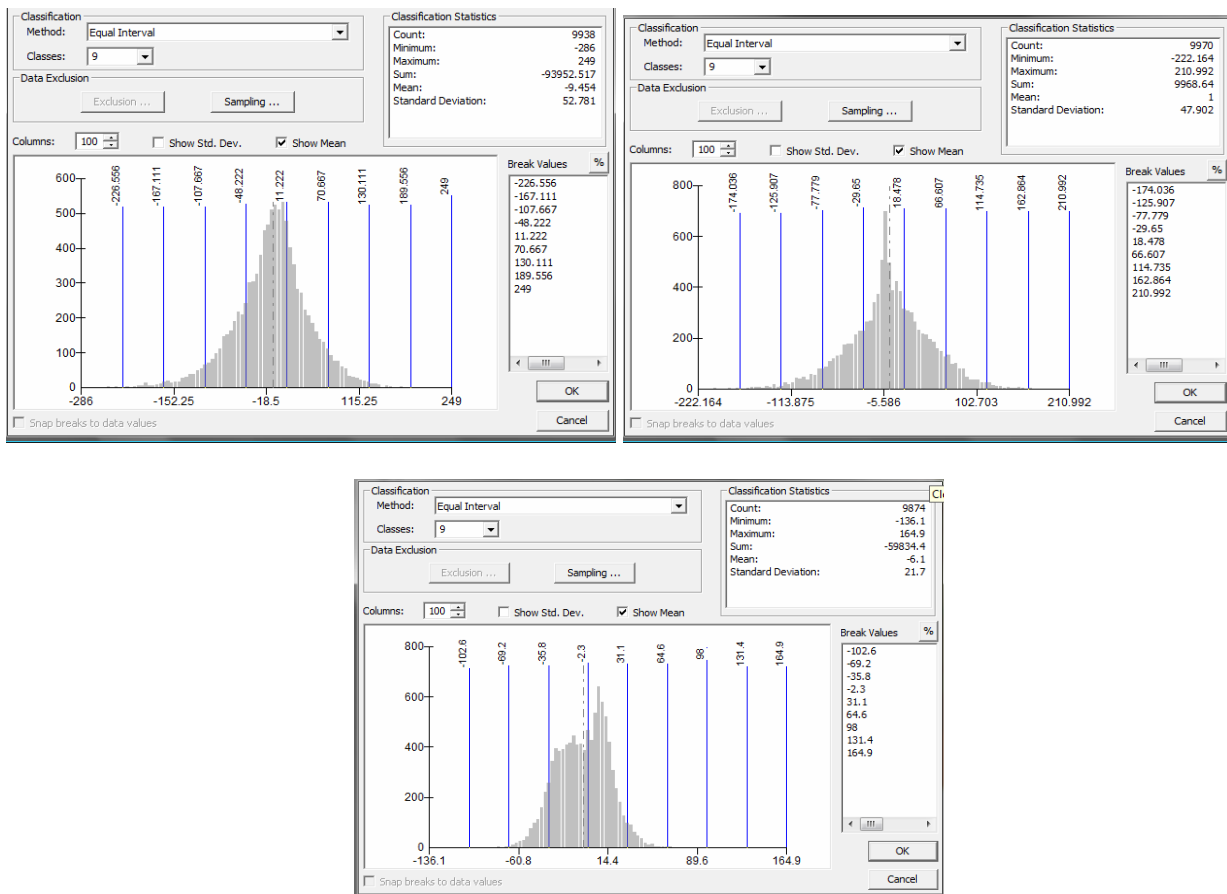
275

Figure 8: Distribution of the differences between the HMGS and SRTM DEM (top left), HMGS and ASTER (top right) and ASTER and SRTM (bottom).

## 3. Hydrological characteristics

The main objective in floodplain analysis is to come to a result of affected areas. For this purpose, hydrological and hydraulic parameters should be estimated and calculated. GIS in collaboration with hydrological models are able to provide many kinds of watershed information and data in GRID format are more frequently and easily used because the store "implicit" topology in condadiction to vector formats [15]. For the hydrological analysis in order to estimate potential flow, data such as: i) slope, ii) aspect, iii) contours, iv) basin areas, and v) flow lines are needed. In this study, these data derived from SRTM and ASTER datasets. Also, contours and flow lines (rivers) from the HMGS maps were digitised in order to produce DEM and raster sets for the comparison with the satellite image data. The HYDROLOGY tool of Spatial Analyst (ArcGIS, ESRI) was used. The procedure was executed three times, one for each different dataset: one time for the SRTM dataset, one for the ASTER dataset and one for the HMGS dataset.

The Hydrology Spatial Analyst Tool provides the algorithms for the creation of sequential raster files for the calculation and visualisation of hydrological parameters. The hydrographic characteristics modeled from all available data sources were: i) network geometry, ii) network classification and iii) watershed delineation. The basic spatial characteristics needed for hydrological analyses that are derived from DEMs:

*(i) Hydrological Basins: determination of drainage basins and sinks within the area of analysis.*

276

    *(ii) Accumulation of Flow: determination of the direction of flow out of each cell for the area of analysis.*

    *(iii) Fill and Sink: correction of the surface raster files remove small-scaled imperfections and sinks.*

    *(iv) Length of flow Lines: calculation of the distance or along a flow path.*

    *(v) Direction of Flow: determination of the direction in which water would flow out of each cell.*

    *(vi) Stream Classification: categorisation by using the Strahler method.*

The aforementioned spatial characteristics are needed for the determination of flow for each basin along with others such as runoff coefficient and Land Characteristics.

### 3.1. Slope and aspect DEM comparisons

The slope and aspect raster results from the ASTER and SRTM are given in Figure 9 and 10 respectively showing the differenced in the total study area. The ASTER slope proved smoother with all values <40% and with better approximation of ground truth in comparison to SRTM slope results. SRTM gave numerous pixel values > 40% of slope that do not respond to the actual relief. The same holds for aspect results with few flat areas (pixel value= -1) that are considered negligible for the scale of the application. The aspect DEM from ASTER 1" in [°] is shown in Figure 11.

### 3.2. Created raster datasets

The dataset created through the procedure described in the previous paragraph are given below. The three different DEMs showed significant variances in watershed (basin) boundaries, due to the different minimum elevation points (pixels) in each raster, providing this way different outflow points (pour points).

The area of the hydrological, in combination with the number of sub-basins divided, reflect to the outflow results. In this case (Figure 12) basins and sub basins on higher elevations are rather similar regardless the DEM used, while the ones on lower elevations have considerable variations
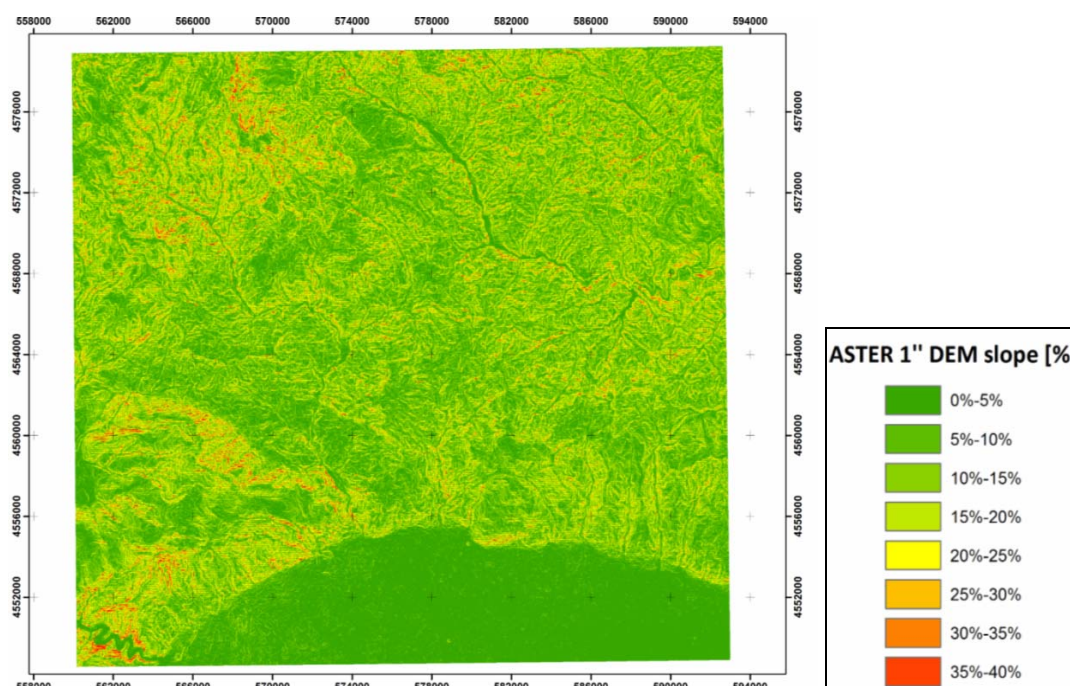


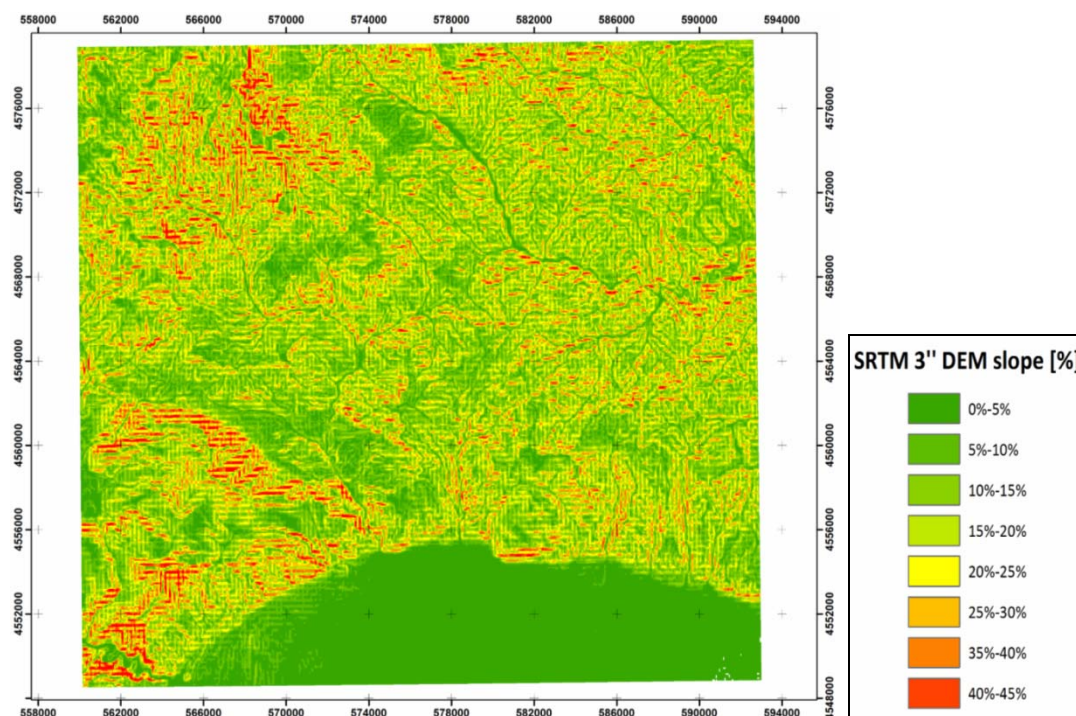Figure 9: Slope in [%] from ASTER 1" DEM.
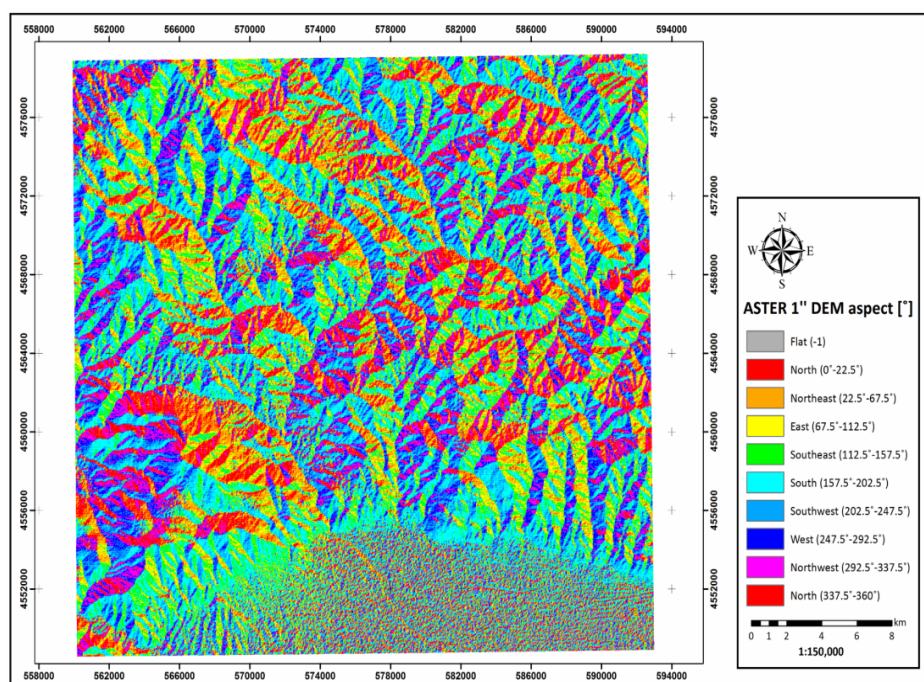
Figure 10: Slope in [%] from SRTM 3" DEM.



Figure 11: Aspect in [°] from ASTER 1" DEM.

terms of numbers of subbasins and their boundaries. Consequently, the hydrographic network derived from each raster gave different spatial data. The hydrographic networks and flow accumulation (Figure 13) from SRTM and ASTER sets were correlated and compared to the one produced by the HMGS maps (local DEM). The hydrographic network from ASTER data shows a better correlation to the one from the local DEM, while the SRTM data gave in some areas distinct poorer results, with several discontinuities but yet considerably reliable if manually corrected (Figure 13).
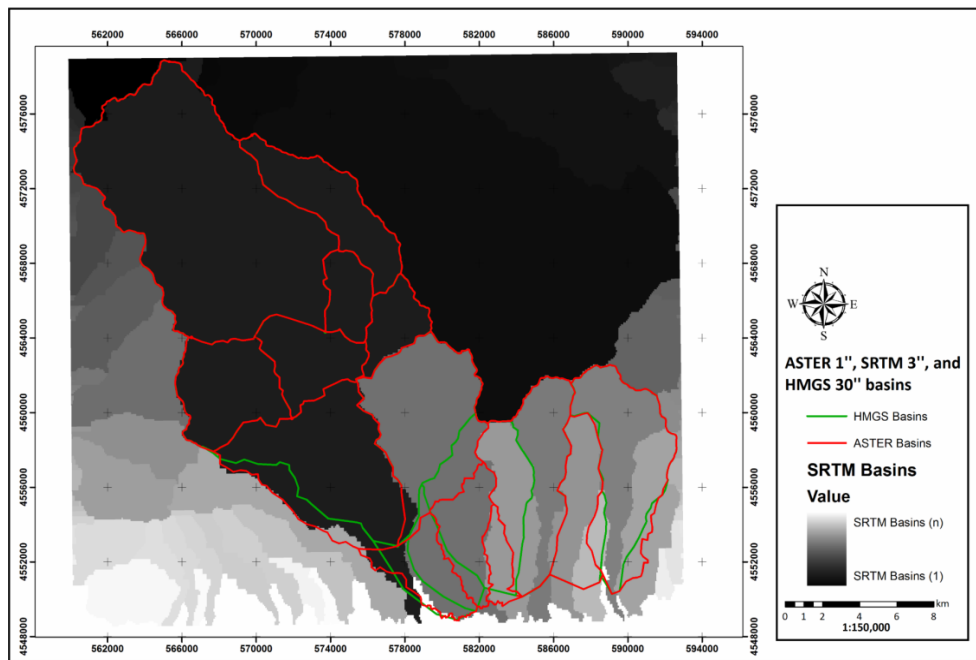
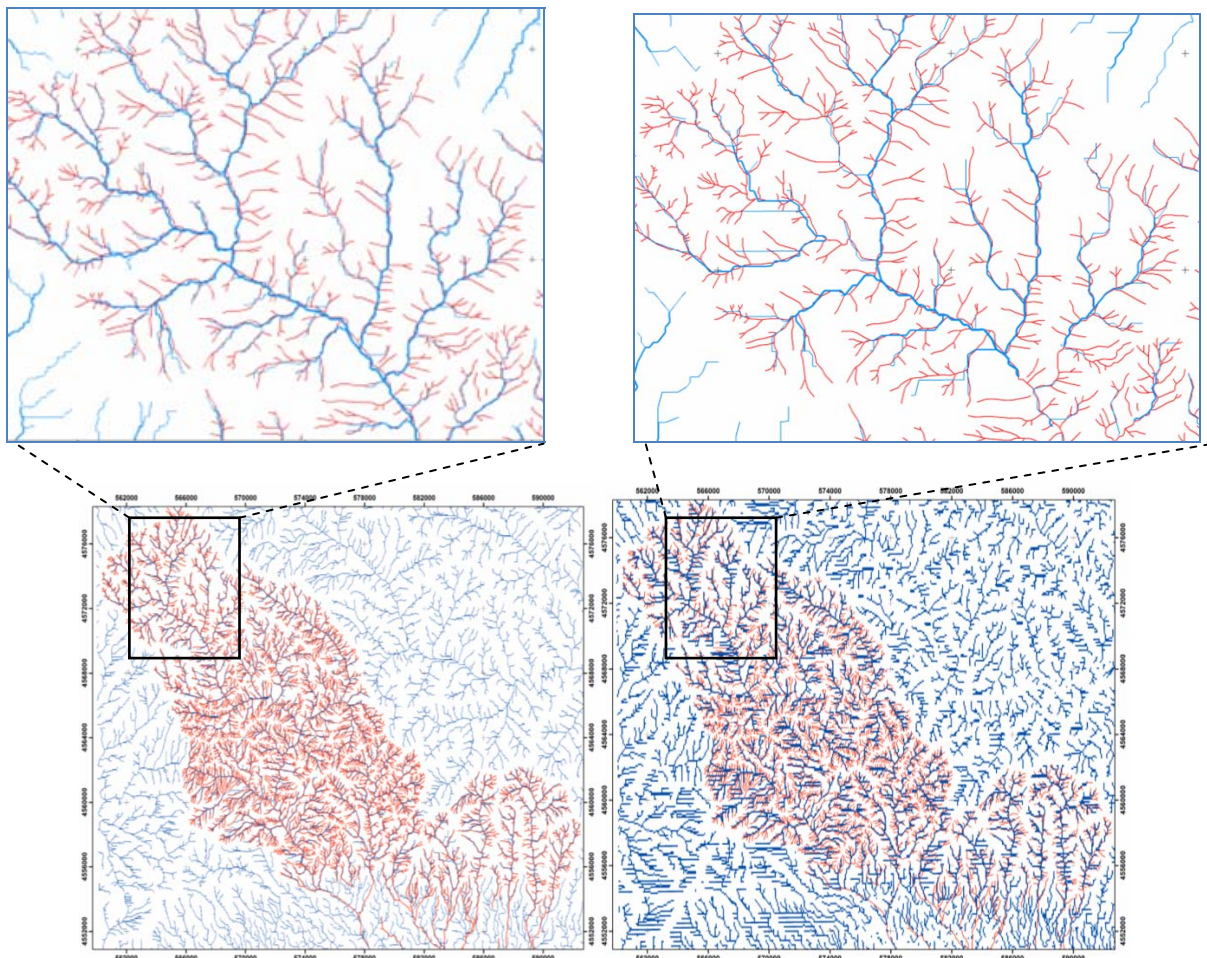Figure 12: Watershed delineation from the available DEMs.



Figure 13: Flow accumulation from ASTER 1" DEM (left) and SRTM 3" DEM (right)
in comparison to local DEM results.

Stream classification was the following procedure occupied for ASTER and SRTM datasets. It proved that SRTM data shower poorer correlation to the local DEM, after the correction procedure used in both cases. ASTER dataset provided a better output in Strahler classification, and corresponds to DEM derived Strahler classification. In both cases the network was classified in class 6 while the network from the SRTM was classified in class 5.

## 4. Hydraulic analysis

Hydraulic analysis in rivers and stream flows is being carried out in order to determine hydraulic flow characteristics. Those of special interest in our case are the ones showing (a) the hydraulic behavior of the stream and (b) the flooding areas. Kosynthos River has given numerous flooding incidents in the past, which in some cases were severe, resulting in flooding areas greater than 20000 $m^2$. Potential Maximun Flow ($Q_{max}$) is needed as an input parameter in river analysis. This parameter was determined by creating an algorithm that uses data derived from the aforementioned procedures as well as empirical and analytical equations. Max Basin Elevation, Min Basin Elevation, Mean Basin Elevation, Flow Length and Basin Area Data were extracted by the processed raster datasets.

The empirical equation of Turazza-Giandotti was used for this study (Eq.1), for evaluating tc: (consentration time, in hrs).

$$t_c = \frac{4 \cdot \sqrt{A} + 1{,}5 \cdot L}{0{,}8 \cdot \sqrt{Z}} \qquad (1)$$

where, A= Basin area-drainage area in $km^2$, L= Flow length (reach length) in km, Z=Mean Basin Elevation-Min Basin Elevation in m.

Concentration time tc is needed for the calculation of maximum flow in the lowest outflow point of a basin. The Max Flow is then calculated based on the following rational equation (Eq. 2).

$$Q = A \cdot i \cdot c \qquad (2)$$

where, Q=Max Flow-peak discharge in $m^3/sec$, A= Basin area-drainage area $m^2$, i: Rainfall Intensity in mm/hr and c=Runoff Coefficient, showing runoff potential. The rainfall intensity equation used for the study area, according is given by the following equation (Eq. 3)

$$i = (22.48 * T^{0,1601}) / t_c^{0.61455} \qquad (3)$$

where, T (rainfall reoccurrence) took the value of 50 (years) of maximum rainfall reoccurrence. Curve number was determined as c=0.5 as a mean value for all basins.

The calculations for estimating peak discharge were executed for each drainage area and each data set respectively in 42 drainage areas separately. The results from each dataset concerning the main basins and sub-basins were then added in order to evaluate maximum discharge flow. The HMGS model gave highest discharge flow (Table 2) and this value was then chosen as the one providing the highest flooding risk for flood simulation.

Maximum flow (Qmax) derived from the different datasets shows significant variations, as expected, that would lead to different flooding characteristics and flooding areas. The HMGS results were chosen to be the input in RiverCAD Professional (Autodesk) in order to analyse and model the hydraulics of water flow through natural rivers and other channels. RiverCAD supports river modeling with a built-in CAD engine using HEC-2 and HEC-RAS software (U.S. Army Corps of Engineers).The geometric data imported in RiverCAD as the land map was derived from field

surveying, in total length of 12.5 km with a surveying zone of 1.1km. The Floodplain Map Analysis gives the option for generating GIS coverages of flooding areas. The coverage was then reintroduced to ArcGIS v9.3 for visualizing the flood areas.

**Table 2**: Nr of basins/sub-basins and estimation of total maximum flow.

| DATASET | NUMBER OF BASINS | SUM | Qmax (m³/sec) |
|---------|------------------|-----|---------------|
| *SRTM* | 8 main basins +7 subbasins | 15 | 845.35 |
| *ASTER* | 5 main basins +8 subbasins | 13 | 887.63 |
| HMGS | 6 main basins +8 subbasins | 14 | 974.72 |

Through hydraulic analysis, floodplain map results were produced as an output. Numeric results are given in tables while flooding geometric characteristics are generated and visualised at channel cross sections and profiles in CAD or GIS as chosen in the output options (Figure 14). The hydraulic model was run in a mixed flow mode that allows subcritical and supercritical flows in one model run.
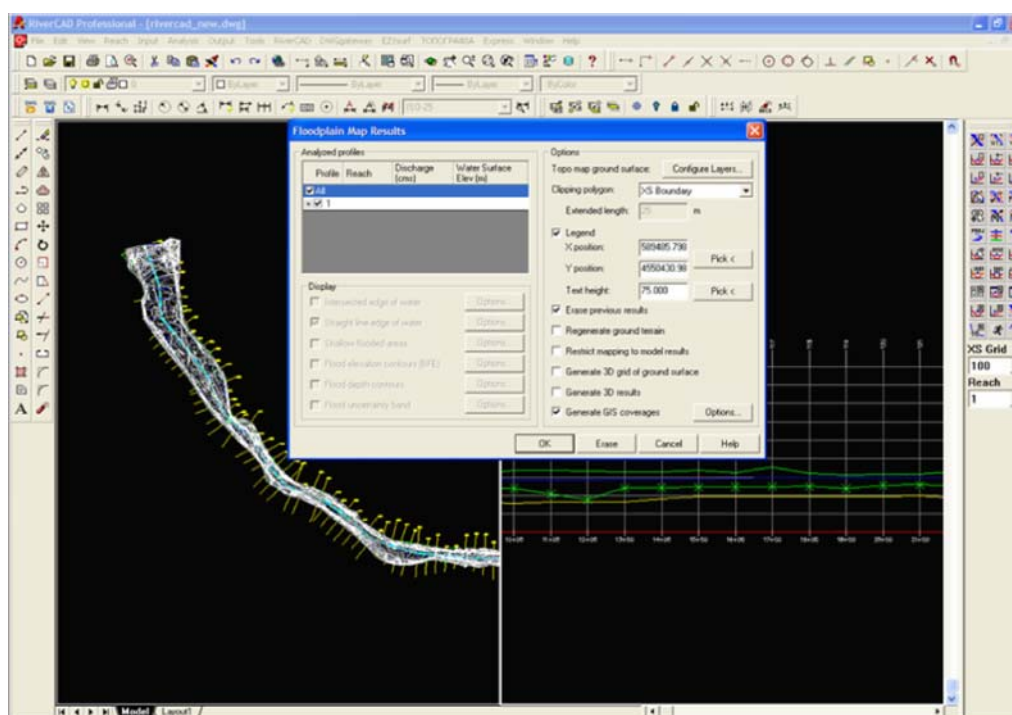


Figure 14: Floodplain analysis and modeling in RiverCAD software.

From the hydraulic analysis it was finally derived that severe flooding occurred in approximately 5km length downstream. In some areas flooding width exceeds 250m from the river banks, with an inundation depth of less than 0.5m (Figure 15), evincing flood hazard zones [7].
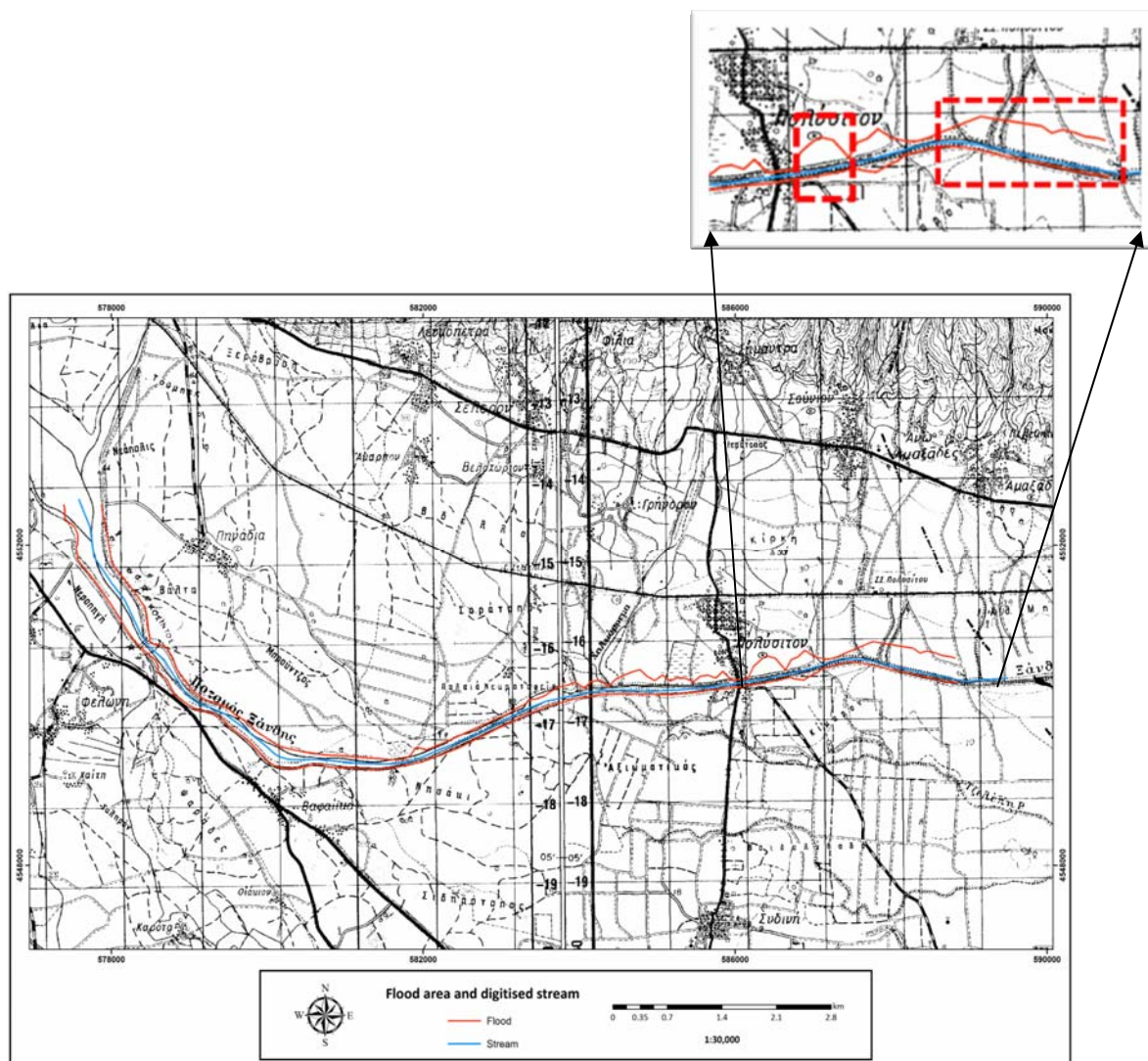
281

Figure 15: Visualization and mapping of flood areas.

## 5. Conclusions

Conclusions from this work were drawn on the adequacy of global digital elevation models for hydrological and hydraulic analysis for river dynamics and flood mapping. This study showed that Global DEMs provide a representation of local topographic features with reasonable agreement compared to the local HMGS model.

The differences of the order of ~47-52m are considered satisfactory given the accuracy of the local DEM itself (estimated at the order of ~10 m).

The derived hydrological characteristics from ASTER and SRTM need to be corrected so that no discontinuities and blunders in the derived features exist.

Satellite global based DEM data can be used for hydrological and hydraulic studies for flood risk assessment, given proper control with local models and field surveying. Though further study ought to be carried out in order to handle errors in DEMs. For accurate river gauge and ground models field surveying provides still the most proper method.

The use of DEM data can prove efficient for mapping flood extends, are relatively easy to obtain and at a reasonable cost. This approach may also be used in large-scale areas were field surveying is time and cost consuming.

## References

[1] Jenson, S. K. and Domingue, J. O., 1988. Extracting topographic structure from digital elevation data for geographical information system analysis. *Photogrammetric Engineering & Remote Sensing*, 54(11): pp. 1593-1600.

[2] Akar, I., 2009. How geographical information systems and remote sensing are used to determine morphometrical features of the drainage network of Kastro (Kasatura) Bay hydrological basin. *International Journal of Remote Sensing*, 30(7): pp. 1737-1748.

[3] Dingman, S. L., 1994. *Physical Hydrology*. Pearson Education Ltd., London, United Kingdom.

[4] Farr, T. G., Rosen, P. A., Caro, E., Crippen, R., Duren, R., Hensley, S., Kobrick, M., Paller, M., Rodriguez, E., Roth, L., Seal, D., Shaffer, S., Shimada, J and Umland, J., 2007. The Shuttle Radar Topography Mission. *Rev Geophys*, 45, RG2004. Doi:10.1029/2005RG000183.

[5] Tarboton, D. G., Bras, R. L. and Rodriguez-Iturbe, I., 1991. On the extraction of channel networks from digital elevation data. *Hydrological Processes*, 5: pp. 81-100.

[6] Farr, T. G. and Kobrick, M., 2000. Shuttle Radar Topography Mission produces a wealth of data. *EOS Trans Amer Geophys Un*, 81: pp. 583-585.

[7] Aigner, H., Hanten. K. P., Stania, K. and Stiefelmeyer, H., 2002. Ausweisung von Naturgefahren – Gefahrenzonenplanung. *Österreichische Wasser- und Abfallwirtschaft* 54 (7-8): pp. 105-109.

[8] Kenward, T., Lettenmaier, D. P., Wood, E. F. and Fielding, E., 2000. Effects of Digital Elevation Model Accuracy on Hydrologic Predictions. *Remote Sensing of Environment*, 74(3): pp. 432-444.

[9] Abrams, M., 2000. The Advanced Spaceborne Thermal Emission and Reflection Radiometer (ASTER): data products for the high spatial resolution imager on NASA's Terra platform. *International Journal of Remote Sensing*, 21(5): pp. 847-859.

[10] Huang, S., Young, C., Feng, M., Heidemann, K., Cushing, W. M., Mushet, D.M. and Liu, S., 2011. Demonstration of a conceptual model for using lidar to improve the estimation of floodwater mitigation potential of Prairie Pothole Region wetlands. *Journal of Hydrology*, 405(3-4): pp. 417-426.

[11] Jenson, S. K., 1991. Applications of Hydrologic Information Automatically Extracted from Digital Elevation Models. *Hydrological Processes*, 5: pp. 31-44.

[12] Liu, X., Peterson, J. and Zhang, Z., 2005. High-Resolution DEM Generated from LiDAR Data for Water Resource Management. In Zerger, A. and Argent, R.M. (eds) MODSIM 2005 International Congress on Modelling and Simulation. Modelling and Simulation Society of Australia and New Zealand, December 2005, pp. 1402-1408. ISBN: 0-9758400-2-9.

[13] Choi, J., Engel, B. A. and Farnsworth, R. L., 2005. Web-based GIS and spatial decision support system for watershed management. *Journal of Hydroinformatics*, 7(3): pp. 165-174.

[14] Strahler, A. N., 1964. Quantitative geomorphology of drainage and channel network, In: Handbook of Applied Hydrology, M. Graw Hill Company, New York.

[15] Bamler, R., 1999. The SRTM Mission: A World-Wide 30 m Resolution DEM from SAR Interferometry in 11 Days. In: Fritsch D and Spiller R (eds) *Photogrametric Week 99*, Wichmann Verlag Heidelberg: pp. 145-154.

[16] Moore, I. D., Grayson, R. B., Ladso, A. R., 2010. Digital terrain modelling: A review of hydrological, geomorphological, and biological applications. *Hydrological Processes*, 5(1): pp. 3-30.

[17] Werner, M., 2001. Shuttle Radar Topography Mission (SRTM), Mission overview. *J* RF-Eng *Telecom* (Frequenz), 55: pp. 75-79.